

Supplemental material for “Quantifying uncertainties and correlations in the nuclear-matter equation of state”

C. Drischler,^{1,2,*} J. A. Melendez,^{3,†} R. J. Furnstahl,^{3,‡} and D. R. Phillips^{4,§}

¹*Department of Physics, University of California, Berkeley, California 94720, USA*

²*Nuclear Science Division, Lawrence Berkeley National Laboratory, Berkeley, California 94720, USA*

³*Department of Physics, The Ohio State University, Columbus, Ohio 43210, USA*

⁴*Department of Physics and Astronomy and Institute of Nuclear and Particle Physics, Ohio University, Athens, Ohio 45701, USA*

(Dated: January 7, 2021)

ADDITIONAL FIGURES

In parallel to the results shown in the main text, we provide here the corresponding figures obtained using the $\Lambda = 450$ MeV potentials.

* cdrischler@berkeley.edu

† melendez.27@osu.edu

‡ furnstahl.1@osu.edu

§ phillid1@ohio.edu

- [1] J. A. Melendez, S. Wesolowski, and R. J. Furnstahl, *Phys. Rev. C* **96**, 024003 (2017), [arXiv:1704.03308](https://arxiv.org/abs/1704.03308).
- [2] C. Drischler, K. Hebeler, and A. Schwenk, *Phys. Rev. Lett.* **122**, 042501 (2019), [arXiv:1710.08220](https://arxiv.org/abs/1710.08220).
- [3] C. Drischler, K. Hebeler, and A. Schwenk, *Phys. Rev. C* **93**, 054314 (2016), [arXiv:1510.06728](https://arxiv.org/abs/1510.06728).
- [4] J. A. Melendez, R. J. Furnstahl, D. R. Phillips, M. T. Pratola, and S. Wesolowski, *Phys. Rev. C* **100**, 044001 (2019), [arXiv:1904.10581](https://arxiv.org/abs/1904.10581).

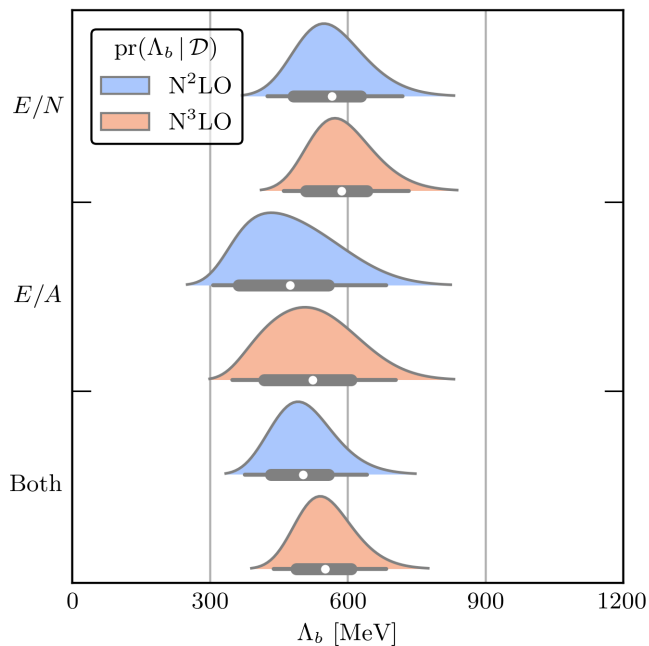


FIG. 1. The analog of Fig. 4 in the main text, but for the $\Lambda = 450$ MeV potentials. The posteriors for the EFT breakdown scale Λ_b using orders through N²LO (blue bands) and N³LO (red bands) corresponding to Fig. 15 in the main text. The upper pair of posteriors comes from analyzing E/N , the middle pair from E/A , and the bottom from a combined analysis. In all cases a Gaussian prior centered at $\Lambda_b = 600 \pm 150$ MeV is used. The combined N³LO posterior is consistent with the $\Lambda_b \approx 600$ MeV found when considering free-space NN scattering observables [1].

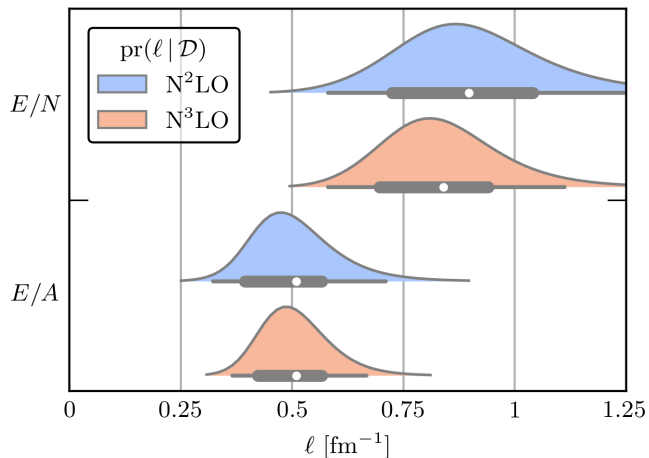


FIG. 2. The analog of Fig. 5 in the main text, but for the $\Lambda = 450$ MeV potentials. Length-scale posteriors organized similarly to Fig. 1. A scale-invariant prior proportional to $1/l$ is used, and each length scale is relative to the k_F of each system. If we were to use a single k_F prescription, the length scales in PNM and SNM, ℓ_{PNM} and ℓ_{SNM} , respectively, would transform just as k_F , making the posteriors shift towards agreement.

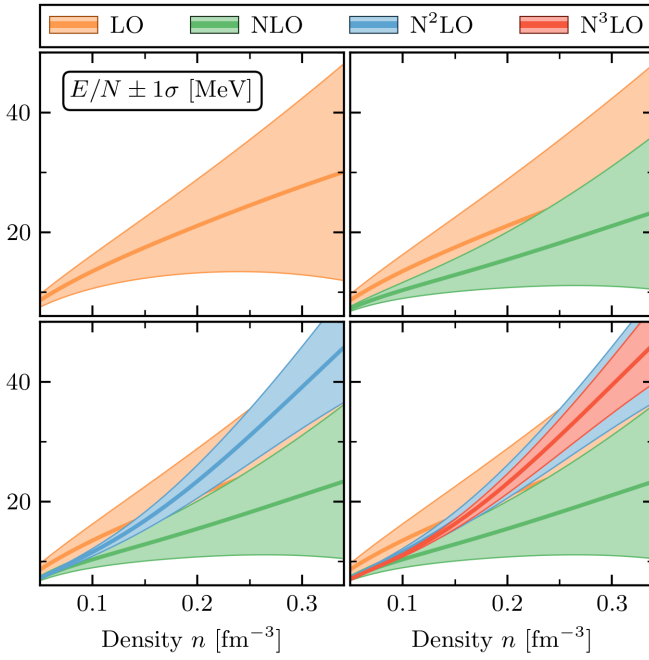


FIG. 3. The analog of Fig. 5 in the main text, but for the $\Lambda = 450$ MeV potentials. The energy per particle in PNM with truncation uncertainties, using a $\Lambda = 450$ MeV potential of Ref. [2]. Bands indicate 68% credible intervals.

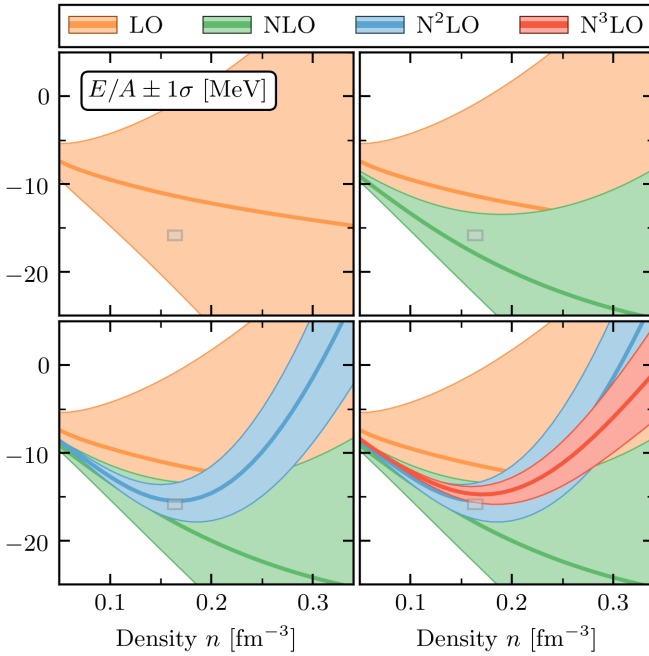


FIG. 4. The analog of Fig. 7 in the main text, but for the $\Lambda = 450$ MeV potentials and similar to Fig. 3 but for SNM. The gray box depicts the empirical saturation point, $n_0 = 0.164 \pm 0.007 \text{ fm}^{-3}$ with $E/A(n_0) = -15.86 \pm 0.57 \text{ MeV}$, obtained from a set of energy-density functionals [2, 3].

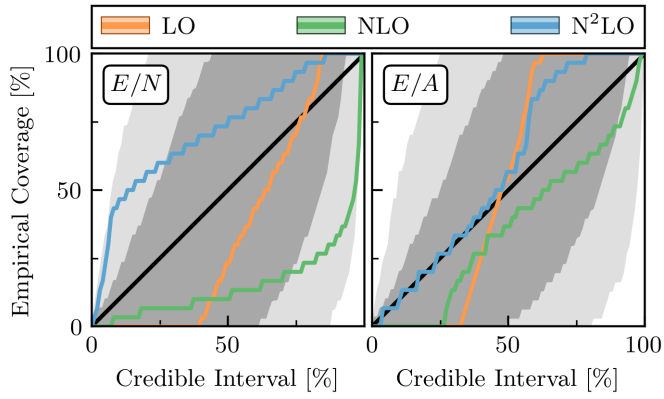


FIG. 5. The analog of Fig. 8 in the main text, but for the $\Lambda = 450$ MeV potentials. Credible-interval diagnostics for the $E/N(n)$ (left-hand side) and $E/A(n)$ uncertainty bands (right-hand side); for details see Ref. [4]. At each order we construct an uncertainty band for the upcoming correction (not the full truncation error) and test whether the next order is contained within it at a specific credible interval. The expected size of fluctuations due to the finite effective sample size of the curves is depicted using dark (light) gray bands for the 68% (95%) interval. Both bands are quite large, which shows that correlations are crucial to assess whether truncation errors have been properly assigned.

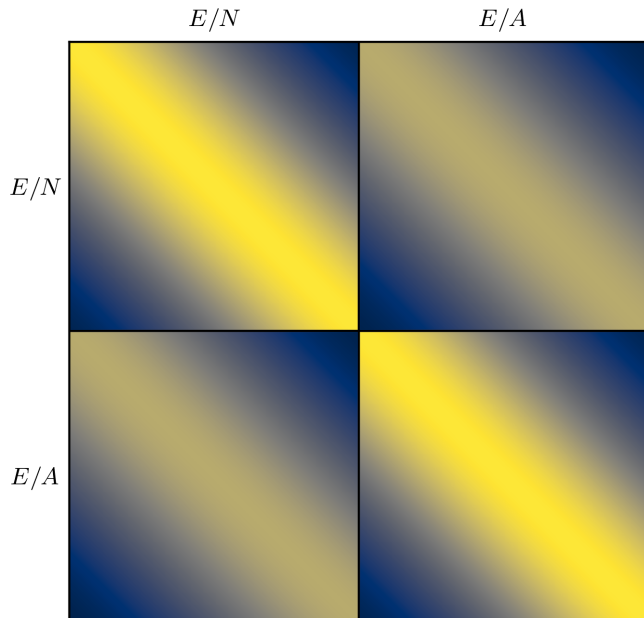


FIG. 6. The analog of Fig. 11 in the main text, but for the $\Lambda = 450$ MeV potentials. Total correlation matrix of $E/N(n)$ and $E/A(n)$ assuming a multitask GP model that was trained to order-by-order results. Each submatrix uses the same grid spaced linearly in k_F . The diagonal blocks show the autocorrelation, and the off-diagonal block is known as the cross correlation. All use RBF kernels. The length scale of the $E/A(n)$ blocks has been transformed to k_F^{PNM} as discussed in the text. Hence, points of equal density between $E/N(n)$ and $E/A(n)$ lie on the diagonal band of the off-diagonal blocks, making them the most highly correlated, but the $E/A(n)$ autocorrelation is unchanged. The length scales were determined by fitting to the $E/N(n)$ and $E/A(n)$ coefficients independently. The correlation $\rho = 0.75$ is a prediction (verified empirically) given these length scales.

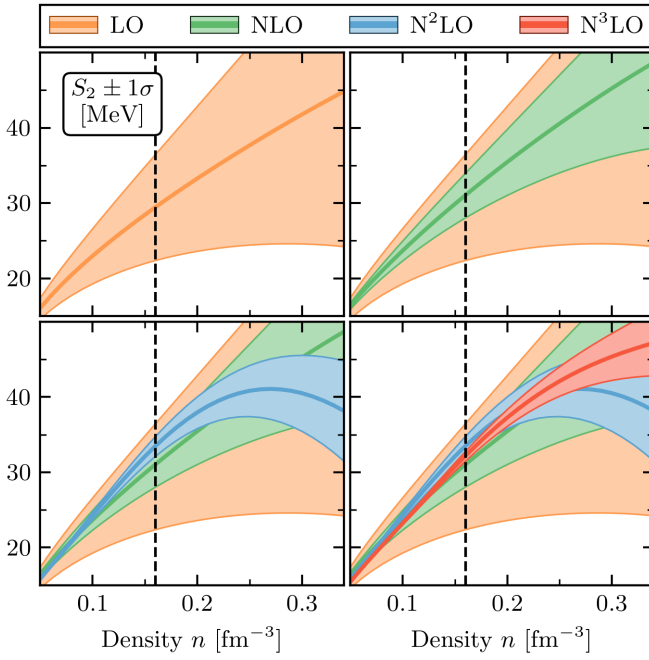


FIG. 7. The analog of Fig. 12 in the main text, but for the $\Lambda = 450$ MeV potentials and similar to Fig. 3, but these are the order-by-order predictions of the symmetry energy $S_2(n)$.

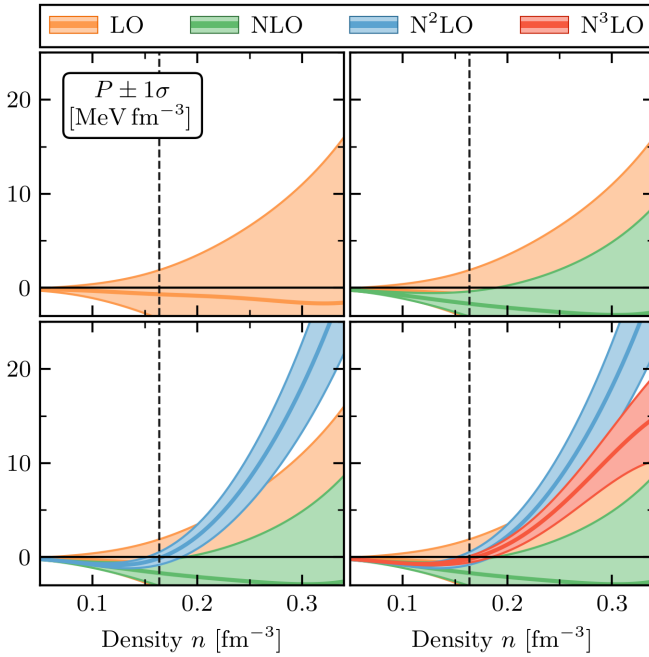


FIG. 8. The analog of Fig. 13 in the main text, but for the $\Lambda = 450$ MeV potentials. Order-by-order predictions of the pressure $P(n)$ of SNM, including differentiation and truncation uncertainty.

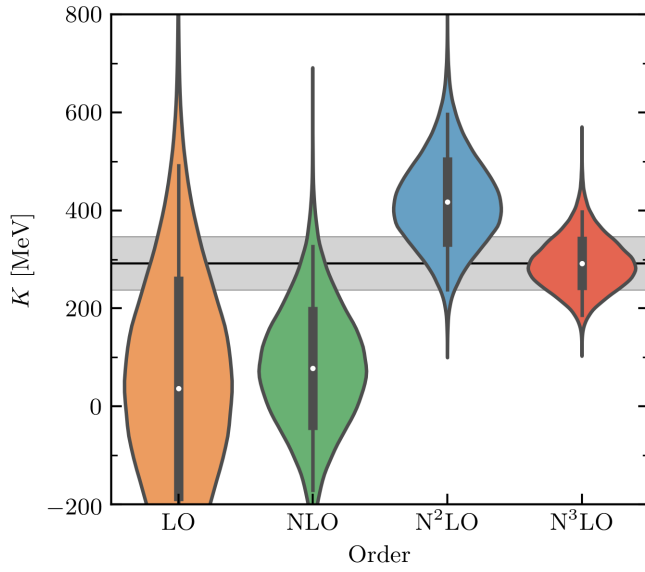


FIG. 9. The analog of Fig. 14 in the main text, but for the $\Lambda = 450$ MeV potentials. Violin plots of the incompressibility K of SNM, shown order-by-order. Curves show the entire smoothed posterior (and its reflection). Each posterior includes differentiation and truncation uncertainty, and are marginalized over all plausible saturation densities $n_0 = 0.17 \pm 0.01 \text{ fm}^{-3}$, see the main text. Dots and bars indicate the mean value, along with the 1σ and 2σ uncertainties. The black line and gray band extends the N^3 LO mean and 1σ uncertainty to more easily compare chiral orders.